Studies of Intermediates in Photoreactions of $Cp_2Fe_2(CO)_4$ with CO and Phosphorus Ligands

Shulin Zhang and Theodore L. Brown*

Contribution from the School of Chemical Sciences, University of Illinois at Urbana Champaign, Urbana, Illinois 61801. *Received May 21, 1992*

Abstract: A combination of flash photolysis with UV–visible and IR detection has been used to study the intermediates in the photochemical reactions of $Cp_2Fe_2(CO)_4$. The reaction kinetics of the intermediates have been investigated using conventional and laser flash photolysis at room temperature. Flash photolyses at low temperatures in hydrocarbon solutions under Ar or CO or in the presence of a phosphorus ligand were carried out for spectral characterizations of the unstable species. A CO-loss intermediate, assigned to the structure $CpFe(\mu\text{-}CO)_2(\mu\text{-}\eta^1,\eta^2\text{-}CO)FeCp$, contains a semibridging CO group. This species is formed in relatively small amounts but is more stable than its structural isomer $CpFe(\mu\text{-}CO)_3FeCp$, a well-established intermediate. A second new intermediate, assigned to $(\eta^5\text{-}Cp)(CO)_2Fe\text{-}Fe(CO)_3(\eta^3\text{-}Cp)$, decays ($k = 5 \times 10^3$ s^{-1} at 22 °C in hexane) to form a third species, assignable to $(\eta^5\text{-}Cp)(CO)Fe(\mu\text{-}\eta^1,\eta^2\text{-}CO)Fe(CO)_2(\eta^3\text{-}Cp)$, which in turn decays ($k = 62.4$ s^{-1} at 25 °C in hexane) to form $Cp_2Fe_2(CO)_4$. The second and third intermediates are formed more extensively under CO. These results provide new evidence for certain previously unexplained features observed on this system. Experiments involving the use of ^{13}CO indicate that formation of the formally 19-electron radical $Cp(CO)_3Fe$ from the 17-electron radical $Cp(CO)_2Fe$ and CO and the subsequent reaction between the two radicals is a major pathway for formation of $(\eta^5\text{-}Cp)(CO)_2Fe\text{-}Fe(CO)_3(\eta^3\text{-}Cp)$ and thus $(\eta^5\text{-}Cp)(CO)Fe(\mu\text{-}\eta^1,\eta^2\text{-}CO)Fe(CO)_2(\eta^3\text{-}Cp)$. Evidence of formation of the two dimer species, even in photolysis under Ar, implies that photoinduced unsymmetrical cleavage of CO bridges in $Cp(CO)Fe(\mu\text{-}CO)_2Fe(CO)Cp$ to afford $Cp(CO)_3Fe$ and $Cp(CO)Fe$ also occurs, in addition to the well-established photoinduced symmetrical cleavage to give two $Cp(CO)_2Fe$. At low temperature, flash photolysis of $Cp_2Fe_2(CO)_4$ in the presence of a phosphorus ligand (L = $P(i\text{-}Pr)_3$, $P(O\text{-}i\text{-}Pr)_3$, $P(OMe)_3$, $P(C_6F_5)_3$) affords evidence of new transient species. The experimental results also support the existence of short-lived precursors to $CpFe(\mu\text{-}CO)_3FeCp$; the latter has previously been considered to be a primary photoproduct via loss of a CO group from $Cp_2Fe_2(CO)_4$.

Introduction

In this contribution we report on observations of new intermediates in the photoreactions of $Cp_2Fe_2(CO)_4$ with CO and phosphorus ligands. The photochemistry of $Cp_2Fe_2(CO)_4$ (**1**) has received a great deal of attention.[1-7] $Cp_2Fe_2(CO)_4$ exists in solutions as cis and trans isomers with bridging CO groups (*cis*-**1**,*trans*-**1**).[8] The isomers undergo rapid interconversion via a nonbridged isomer (non-**1**) present in trace concentration.[8,9] Several intermediates (**2**–**5**) have been observed or proposed in the photochemical reactions of the dimer complex. These are summarized in Scheme I.

Scheme I

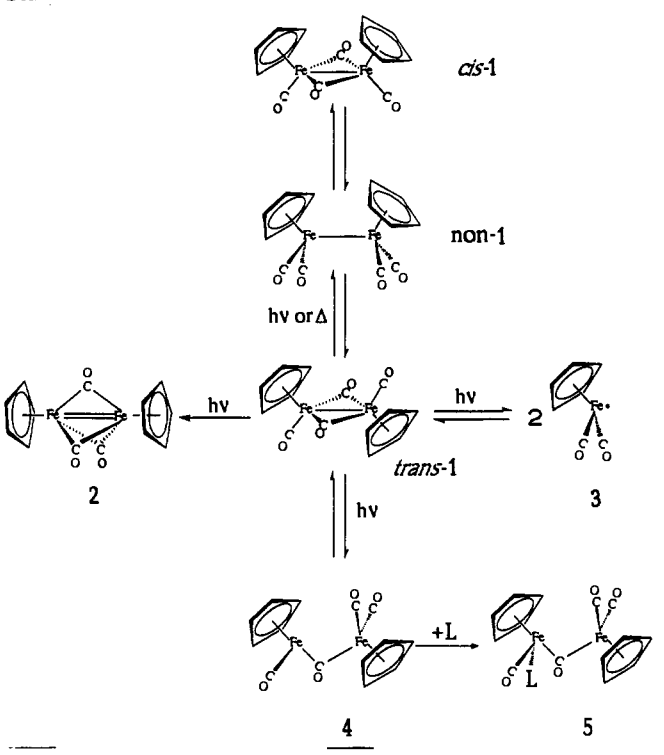

(1) (a) Geoffroy, G. L.; Wrighton, M. S. *Organometallic Photochemistry*; Academic Press: New York, 1979. (b) Abrahamson, H. B.; Palazzotto, M. C.; Reichel, C. L.; Wrighton, M. S. *J. Am. Chem. Soc.* **1979**, *101*, 4123. (c) Hepp, A. F.; Blaha, J. P.; Lewis, C.; Wrighton, M. S. *Organometallics* **1984**, *3*, 174.

(2) (a) Caspar, J. V.; Meyer, T. J. *J. Am. Chem. Soc.* **1980**, *102*, 7794. (b) Meyer, T. J.; Caspar, J. V. *Chem. Rev.* **1985**, *85*, 187.

(3) (a) Tyler, D. R.; Schmidt, M. A.; Gray, H. B. *J. Am. Chem. Soc.* **1979**, *101*, 2753. (b) Tyler, D. R.; Schmidt, M. A.; Gray, H. B. *J. Am. Chem. Soc.* **1983**, *105*, 6018. (c) Goldman, A. S.; Tyler, D. R. *Inorg. Chem.* **1987**, *26*, 253. (d) Castellani, M. P.; Tyler, D. R. *Organometallics* **1989**, *8*, 2113. (e) Tyler, D. R. In *Organometallic Radical Processes*; Trogler, W. C., Ed.; Elsevier: Amsterdam, 1990; p 338.

(4) (a) Moore, B. D.; Simpson, M. B.; Poliakoff, M.; Turner, J. J. *J. Chem. Soc., Chem. Commun.* **1984**, 972. (b) Moore, B. D.; Simpson, M. B.; Poliakoff, M.; Turner, J. J. *J. Phys. Chem.* **1985**, *89*, 850. (c) Dixon, A. J.; Healy, M. A.; Poliakoff, M.; Turner, J. J. *J. Chem. Soc., Chem. Commun.* **1986**, 994. (d) Moore, B. D.; Poliakoff, M.; Turner, J. J. *J. Am. Chem. Soc.* **1986**, *108*, 1819. (e) Dixon, A. J.; Healy, M. A.; Hodges, M. P.; Moore, B. D.; Poliakoff, M.; Simpson, M. B.; Turner, J. J.; West, M. A. *J. Chem. Soc., Faraday Trans.* **1986**, *82*, 2083. (f) Dixon, A. J.; Gravelle, S. J.; van de Burgt, L. J.; Poliakoff, M.; Turner, J. J.; Weitz, E. *J. Chem. Soc., Chem. Commun.* **1987**, 1023. (g) Dixon, A. J.; George, M. W.; Hughes, C.; Poliakoff, M.; Turner, J. J. *J. Am. Chem. Soc.* **1992**, *114*, 1719.

(5) (a) Hooker, R. H.; Mahmoud, K. A.; Rest, A. J. *J. Chem. Soc., Chem. Commun.* **1983**, 1022. (b) Hooker, R. H.; Rest, A. J. *J. Chem. Soc., Dalton Trans.* **1990**, 1221. (c) Bloyce, P. E.; Campen, A. K.; Hooker, R. H.; Rest, A. J.; Thomas, N. R.; Bitterwolf, T. E.; Shade, J. E. *J. Chem. Soc., Dalton Trans.* **1990**, 2833.

(6) (a) Moore, J. N.; Hansen, P. A.; Hochstrasser, R. M. *J. Am. Chem. Soc.* **1989**, *111*, 4563. (b) Anfinrud, P. A.; Han, C.-H.; Lian, T.; Hochstrasser, R. M. *J. Phys. Chem.* **1991**, *95*, 574.

(7) (a) Bursten, B. E.; Cayton, R. H. *J. Am. Chem. Soc.* **1986**, *108*, 8241. (b) Bursten, B. E.; McKee, S. D.; Platz, M. S. *J. Am. Chem. Soc.* **1989**, *111*, 3428.

(8) (a) Manning, A. R. *J. Chem. Soc. A* **1968**, 1319. (b) McArdle, P. A.; Manning, A. R. *J. Chem. Soc. A* **1969**, 1948.

(9) (a) Bullitt, J. G.; Cotton, F. A.; Marks, T. J. *J. Am. Chem. Soc.* **1970**, *92*, 2155. (b) Gansow, O. A.; Burke, A. R.; Vernon, W. D. *J. Am. Chem. Soc.* **1972**, *94*, 2550. (c) Gansow, O. A.; Burke, A. R.; Vernon, W. D. *J. Am. Chem. Soc.* **1976**, *98*, 5817.

0002-7863/93/1515-1779$04.00/0

$Cp_2Fe_2(CO)_4$ has been shown to undergo photochemical substitution of a carbonyl group by phosphines or phosphites.[10] Tyler, Schmidt, and Gray first presented evidence that the substitution reaction with $P(O\text{-}i\text{-}Pr)_3$ proceeds via an intermediate ($Cp(CO)_2Fe\text{-}C(O)\text{-}Fe(CO)Cp$) in which a single CO bridges the Fe atoms and there is no direct Fe–Fe bond.[3a,b] Wrighton and co-workers examined the reaction of PPh_3 with $Cp_2Fe_2(CO)_4$ in the presence of halide donors such as CCl_4 or $1\text{-}IC_5H_{11}$ and found that formation of $Cp_2Fe_2(CO)_3PPh_3$ is suppressed due to formation of $Cp(CO)_2FeCl$ or $Cp(CO)_2FeI$.[1b] They proposed that the substitution reaction takes place through the radical intermediate. Caspar and Meyer detected two distinct species, consistent with $Cp(CO)_2Fe^{\bullet}$ and $Cp_2Fe_2(CO)_3$, by using UV–visible spectroscopy following flash photolysis of $Cp_2Fe_2(CO)_4$ in solutions.[2a] They argued that the CO-loss intermediate $Cp_2Fe_2(CO)_3$ is responsible for the formation of the monosubstituted product $Cp_2Fe_2(CO)_3PPh_3$; $Cp(CO)_2FeCl$ can be formed through reaction of CCl_4 with either $Cp(CO)_2Fe^{\bullet}$ or $Cp_2Fe_2(CO)_3$.

$Cp_2Fe_2(\mu\text{-}CO)_3$ was first independently observed in polyvinyl chloride films and methane matrices at 12 K[5a] and in organic glasses at 77 K[1c] by using IR and UV–visible detection methods. It has been demonstrated that the symmetrically bridged species **2** is formed exclusively from *trans*-**1** in low-temperature matrices or organic glasses. The mechanism for formation of **2** remains obscure, although it has been suggested that the loss of CO and rearrangement to form the $(\mu\text{-}CO)_3$ structure from *trans*-**1** is a concerted process.[1c] Both $Cp(CO)_2Fe^{\bullet}$ and $Cp_2Fe_2(\mu\text{-}CO)_3$ have been identified in solutions at room temperature by employing fast time-resolved IR spectroscopy after flash photolysis of $Cp_2Fe_2(CO)_4$.[4] Wrighton and co-workers have reported the isolation and characterization of $Cp^*_2Fe_2(\mu\text{-}CO)_3$ ($Cp^* = C_5Me_5$), an analogue of $Cp_2Fe_2(\mu\text{-}CO)_3$.[11] As a result of its symmetrical bridging structure, the compound possesses a triplet ground state.

More recently, Rest and co-workers demonstrated that low-energy photolysis ($\lambda > 475$ nm at 12 K) results in bridge opening of the trans-bridged species (*trans*-$Cp(CO)Fe(\mu\text{-}CO)_2Fe(CO)Cp$) to form an all-terminal structure,[5c] which they propose is responsible for the intermediate $(Cp(CO)_2Fe\text{-}C(O)\text{-}Fe(CO)Cp)$ observed by Tyler et al. at −78 °C.[3a,b] They confirm that high-energy photolysis ($320 < \lambda < 390$ nm) results in the reaction of only the trans isomer and that neither the radical **3** nor **2** is formed photochemically from *cis*-**1**.

The role of intermediates such as **4** in substitution reactions has been questioned recently by Hochstrasser and co-workers.[6] According to their experiments using femtosecond time-resolved IR spectroscopy, any nonbridged or single-CO-bridged species has a lifetime shorter than 20 ps. It is therefore considered unlikely for such intermediates to react with incoming ligands through bimolecular collisions.

The reactivity of $Cp(CO)_2Fe^{\bullet}$ (**3**) has been studied using flash photolysis with UV–visible or IR detection. It recombines rapidly ($k \approx 3 \times 10^9$ M^{-1} s^{-1} in cyclohexane at 22 °C) to re-form **1**[2a] and also undergoes rapid substitution by $P(OMe)_3$ to form $Cp(CO)FeP(OMe)_3$ ($k \approx (8.9 \pm 2.0) \times 10^8$ M^{-1} s^{-1} in *n*-heptane at 25 °C).[4c] However, **3** appears to react more slowly with PPh_3, PBu_3, or CH_3CN.[4f] The kinetics and mechanism of reactions of **2** with various nucleophiles to generate the monosubstituted product $Cp_2Fe_2(CO)_3L$ also have been studied using flash photolysis methods.[2a,4c,7b,12]

We have investigated the photochemistry of **1** in hydrocarbon solutions using conventional xenon lamp flash and laser flash photolyses at both room temperature and low temperatures. We present here the evidence for three new intermediates recently reported in a communication[13] and some observations on flash photolysis of **1** in the presence of a few phosphorus ligands at low temperatures. After the experiments reported here had been completed, a report by Poliakoff, Turner, and co-workers of the photochemical substitution reactions of $Cp_2Fe_2(CO)_4$ in hydrocarbon and THF solution appeared.[4g] Using time-resolved IR spectroscopy at room temperature, these authors found evidence for $Cp_2Fe_2(CO)_3(THF)$ following UV and visible flash photolysis, formation of which involves neither $Cp(CO)_2Fe^{\bullet}$ nor $Cp_2Fe_2(\mu\text{-}CO)_3$ as precursors. Substitution by phosphites was shown to proceed via substitution of the $Cp(CO)_2Fe^{\bullet}$ radical or addition to **2**. The results from this work and our own overlap on some points; more importantly, they are complementary to one another on several important questions.

Experimental Section

All experiments were carried out under an atmosphere of purified argon employing Schlenk techniques or were performed in a glovebox with an Ar atmosphere. Infrared spectra were recorded on a Perkin-Elmer 1710 FTIR spectrometer. A 1.0-mm KCl solution cell with Teflon-brand stopcocks was employed for measurements at room temperature. For low-temperature measurements, a SPECAC Model 21500 variable-temperature system was employed. The cell consists of CaF_2 windows and lead spacer with a pathlength of 1-mm. The jacket windows for the SPECAC system are KBr or CaF_2 plates. UV–visible spectra were taken on a Hewlett-Packard HP8452 spectrometer (190–820 nm) using 1-cm-pathlength quartz cells with Teflon-brand stopcocks or the above-mentioned CaF_2 cell for low-temperature measurements.

$Cp_2Fe_2(CO)_4$ (Strem Chemicals) was used without further purification. Purification procedures for *n*-hexane (Burdick and Jackson) and carbon monoxide (Matheson Gas Products, Matheson purity grade, 99.99+%) have been described previously.[14] Carbon-13 monoxide, obtained from Monsanto Research Corporation and containing 99.58% ^{13}C and 17.75% ^{18}O, was purified using the same procedures as for CO. Methylcyclohexane (MCH, 99%) and 3-methylpentane (3MP, 99+%) from Aldrich were distilled over CaH_2 and stored in flasks containing freshly activated 4-Å molecular sieves. MCH and 3MP were subjected to three cycles of free–pump–thaw degassing prior to use. $P(O\text{-}i\text{-}Pr)_3$ and $P(OMe)_3$ (Aldrich) were distilled over CaH_2. $P(i\text{-}Pr)_3$ from Strem Chemicals in a sealed ampule tube and $P(C_6F_5)_3$ from Aldrich were opened in the glovebox and used as received.

The flash photolysis measurements were carried out as described previously.[14,15b,16] The conventional flash photolysis apparatus is comprised of two linear high-pressure xenon-flash tubes. The probe beam is provided by an Ushio quartz-halogen-tungsten filament lamp (100 W). For experiments in which it was necessary to attenuate the probe beam intensity, various metal wire screens were inserted into the beam path in front of the flash cell. The relative probe beam intensity was determined through the voltage output of the photomultiplier tube. A nitrogen laser (337 nm) was employed in laser flash photolysis. For continuous photolysis reactions, a 275-W GE sunlamp which produces predominantly 366-nm irradiation was used.

To obtain IR or UV–visible spectra of a solution after flash photolysis, the IR cell or quartz cell containing the reaction solution was placed facing the xenon-flash tubes (5 cm away). Following photolysis the cell was immediately moved to the spectrometer. For IR measurements, typically four scans were collected for each spectrum with 2-cm^{-1} resolution, which took about 1 min.

Results and Discussion

A. Observation of a Long-Lived Species (6). Xenon lamp flash photolysis of a hexane solution of **1** at room temperature under Ar results in the appearance of **2** ($\lambda_{max} = 510$ nm),[2a] which decays with second-order kinetics. However, the absorbance does not return to the preflash value within 8 s. The difference IR spectra before and after flash photolysis are shown in Figure 1. In this time domain, **2** has disappeared, as evidenced by the absence of a band at about 1820 cm^{-1} due to $(\mu\text{-}CO)_3$.[1c,4,5] However, the spectra reveal negative absorbance due to **1** and three new bands at 1839, 1786, and 1674 cm^{-1} (Figure 1a), which disappear over

(10) (a) Mills, O. S. *Acta Crystallogr.* **1958**, *11*, 620. (b) Haines, R. J.; Du Preez, A. L. *Inorg. Chem.* **1969**, *8*, 1459. (c) Giannotti, C.; Merle, G. *J. Organomet. Chem.* **1976**, *105*, 97. (d) Labinger, J. A.; Madhaven, S. *J. Organomet. Chem.* **1977**, *134*, 381.

(11) Blaha, J. P.; Bursten, B. E.; Dewan, J. C.; Frankel, R. B.; Randolph, C. W.; Wilson, B. A.; Wrighton, M. S. *J. Am. Chem. Soc.* **1985**, *107*, 4561.

(12) Zhang, S.; Brown, T. L. *Organometallics* **1992**, *11*, 4166.

(13) Zhang, S.; Brown, T. L. *J. Am. Chem. Soc.* **1992**, *114*, 2723.

(14) Zhang, S.; Dobson, G. R.; Brown, T. L. *J. Am. Chem. Soc.* **1991**, *113*, 6908.

(15) (a) Sullivan, R. J.; Brown, T. L. *J. Am. Chem. Soc.* **1991**, *113*, 9155. (b) Sullivan, R. J.; Brown, T. L. *J. Am. Chem. Soc.* **1991**, *113*, 9162. (c) Zhang, S.; Brown, T. L. *Organometallics* **1992**, *11*, 2122.

(16) Herrick, R. S.; Herrinton, T. R.; Walker, H. W.; Brown, T. L. *Organometallics* **1985**, *4*, 42.

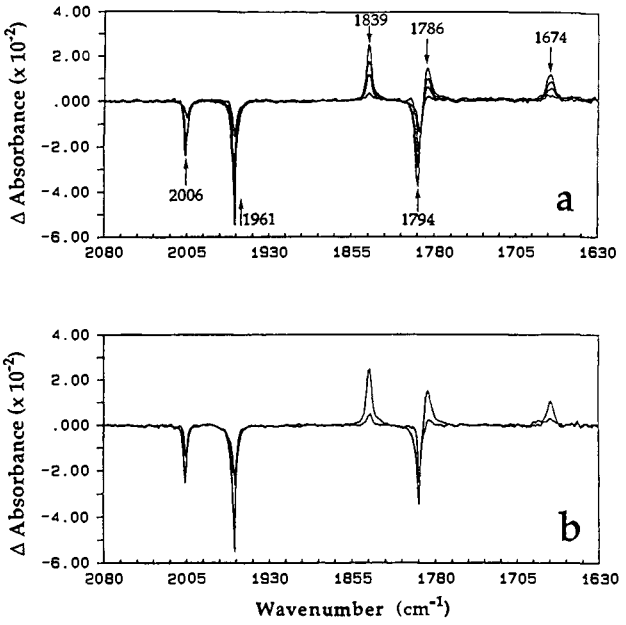

Figure 1. Difference IR spectra of $Cp_2Fe_2(CO)_4$ (1.7 mM) in hexane under Ar in a 1.0-mm KCl cell. The spectrum before flash is subtracted from the spectra after the flashes. (a) Various times after seven flashes; the succesive spectra represent 1, 30, 60, and 150 min following the flashes. (b) The outside spectrum represents 1 min after seven flashes, and the inside spectrum represents 8 min of sunlamp irradiation followed by an additional delay of 22 min after seven flashes.

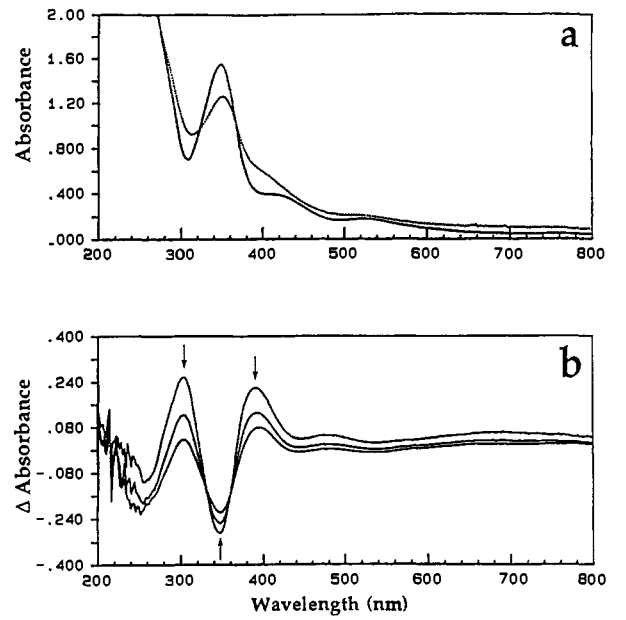

Figure 2. (a) UV-visible spectra of a hexane solution of $Cp_2Fe_2(CO)_4$ (0.15 mM) under Ar before (—) and 1 min after (···) seven flashes in a 10-mm quartz cell. (b) The difference spectra before and after the seven flashes (1, 60, and 180 min, respectively).

2–3 hours. The spectral changes with time show that the new species, designated **6**, decays to form **1**. Bands due to **6** were seen after a single flash of the solution; seven consecutive flashes at 40-s intervals resulted in accumulation of more **6** (~4-fold increase) without producing any other product. The UV-visible spectrum of the solution taken within 30 s following the flash reveals that the long-lived species has increased absorbance throughout the visible region (Figure 2). Because the starting material absorbs strongly in the 300–400-nm range, it is difficult to ascertain whether **6** has an absorption maximum in this region, but it appears likely that there is a broad band in this region.

Sunlamp photolysis of **1** does not produce **6**. As shown in Figure 1b, when **6** is first produced via xenon lamp flashes and subsequently irradiated by a sunlamp, its decay is accelerated. The IR spectrum of **6** is consistent with an unsymmetrical bridging species; the low-energy band at 1674 cm^{-1} is most likely due to a linear semibridge CO. Making allowance for the presence of an additional terminal CO on each metal in the Mo species, the observed pattern of bands is closely similar to that ascribed to $Cp_2Mo_2(CO)_2(\mu\text{-}CO)_2(\mu\text{-}\eta^1,\eta^2\text{-}CO)$ (1978, 1933, 1898, 1855, and 1665 cm^{-1}).[5b,17]

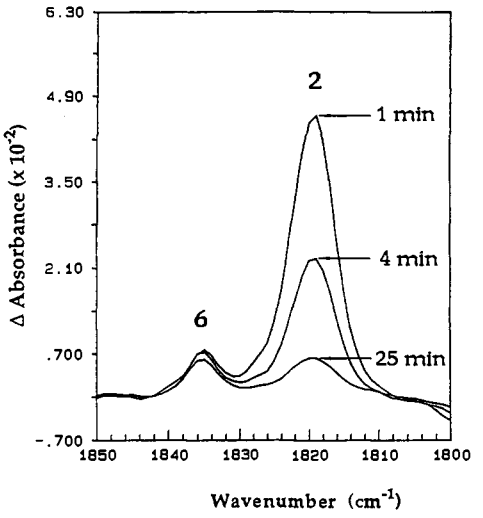

Figure 3. IR spectra of a solution of $Cp_2Fe_2(CO)_4$ (1.7 mM) in MCH–3MP (9:1) under Ar after seven flashes in a 1.0-mm CaF_2 cell at −25 °C.

The long-lived CO-loss species **6** is formed in relatively small amounts compared to its well-known isomer **2**. This is probably the main reason why it was not noticed previously. Indeed, close examination of the time-resolved IR spectra at room temperature in cyclohexane, reported by Poliakoff, Turner, and co-workers,[4a] seems to suggest that a band at 1839 cm^{-1} exists as a weak shoulder to the peak at 1823 cm^{-1} due to **2**. The other two bands for **6** are not seen in their time-resolved spectra, presumably because of their low intensity and the limited spectral range observed (2050–1700 cm^{-1}), as well as the limited resolution (maximum 4 cm^{-1}).

6 is considerably less reactive toward CO than its isomer **2** or other semibridging species for which observations of reactivity have been made, e.g., $Mn_2(CO)_8(\mu\text{-}\eta^1,\eta^2\text{-}CO)$.[15] In the time regime of 30 s to minutes, **6** is not observed following flash photolysis of solutions under 1 atm of CO. In the presence of $HSnBu_3$ (15 mM), $HSiEt_3$ (500 mM), 1-hexene (80 mM), or H_2O (saturated), however, the decay of **6** is nearly unaffected, indicating its low reactivity toward these reagents. Much higher reactivities have been observed for **2** and $Mn_2(CO)_8(\mu\text{-}\eta^1,\eta^2\text{-}CO)$ toward $HSnBu_3$.[15]

Visible light irradiation probably excites **6** so as to open the semibridge or transform it into a symmetric bridge (i.e., **6** → **2**), permitting faster reaction with CO. Thus the efficient secondary photolysis by visible irradiation prevents accumulation of **6** during photolysis of **1**.

Low-temperature IR experiments rule out the possibility of **6** being formed from **2**. Figure 3 shows the IR bands at 1819 and 1836 cm^{-1} due to **2** and **6**, respectively, after flash photolysis of **1** in MCH–3MP (9:1) under Ar at −25 °C. Clearly, the disappearance of **2** is not accompanied by a growth of **6**. There is no conclusive evidence in our experiments for formation of **6** at −180 °C in the organic glass after flash photolysis; under these conditions only **2** was observed. Our inability to observe **6** was originally thought to be due to broadening of the IR bands at the lower temperature. However, additional experiments ruled out this possibility, since **6** is still observable at −180 °C when first generated at room temperature and then immediately cooled down to −180 °C. We postulate that **6** is produced via a radical pathway

(17) Hooker, R. H.; Mahmoud, K. A.; Rest, A. J. *J. Organomet. Chem.* **1983**, *254*, C25.

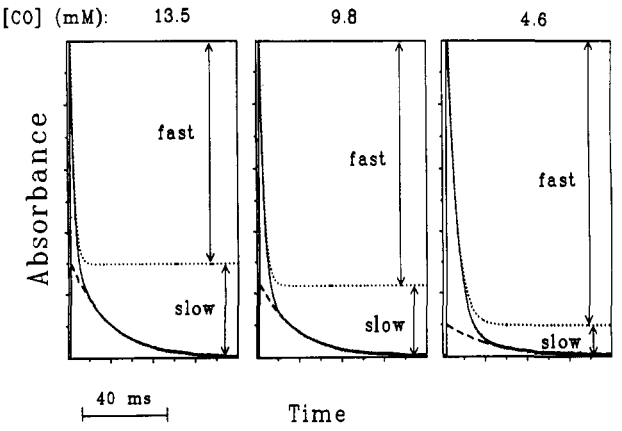

Figure 4. Absorbance (normalized) vs time fitted as a sum of two exponential functions on the signal obtained at 510 nm after xenon-tube flash photolysis of $Cp_2Fe_2(CO)_4$ (3×10^{-5} M) in hexane at 25 °C under various CO partial pressures.

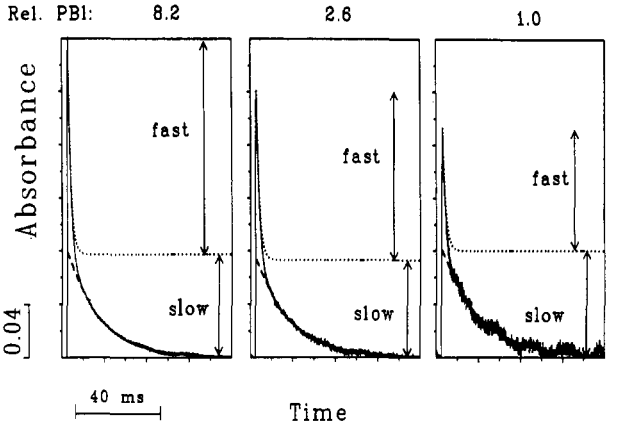

Figure 5. Absorbance vs time fitted as a sum of two exponential functions on the signal obtained at 510 nm after xenon-tube flash photolysis of $Cp_2Fe_2(CO)_4$ (3×10^{-5} M) in hexane under 1 atm of CO at 25 °C when various probe beam intensities were used.

through reaction of $Cp(CO)_2Fe$ with Cp(CO)Fe. Failure to observe **6** at −180 °C is probably due to a strong cage effect, i.e., radicals derived from **1** rapidly recombine before undergoing subsequent reactions. $Cp(CO)_2Fe$ and Cp(CO)Fe may be generated via symmetrical fragmentation and unsymmetrical cleavage from **1**. This process will be further discussed in detail in sections D and G.

B. Flash Photolysis of 1 under CO at Room Temperature. Flash photolysis of **1** under CO in cyclohexane has been studied by Caspar and Meyer[2a] and by Turner et al.[4c] using visible and IR detections, respectively. Transient absorbance decays, observed in the time regions from 200 μs to 100 ms and obeying first-order kinetics, were attributed to the reaction of **2** with CO. In our experiments employing conventional flash photolysis with monitoring at 510 nm, we observed two exponential decays. The rate constants under 1 atm of CO ([CO] = 13.5 mM),[18] corresponding to two first-order processes, are 750 and 60 s^{-1}, respectively. Varying the concentration of CO through the use of CO/Ar cover gas mixtures and assuming that Henry's law applies, we found that the rate constant for the faster decay is proportional to [CO], whereas that for the slower decay is independent of [CO], $k_{slow} = 62.5 \pm 1.5$ s^{-1}. The observed faster and slower processes are attributed, respectively, to the reaction of **2** and a new species (**7**) to form **1**.

The concentration of **7** increases with CO partial pressure over the solution although the rate of its decay is unaffected by [CO]. These points are demonstrated in Figure 4, where the total absorbance change (normalized) is resolved into two exponential functions. It is seen that the portion of absorbance change associated with the slow process, and thus attributable to **7**, decreases as [CO] decreases. Surprisingly, it was also noted that the magnitude of absorbance change due to the faster process **2** → **1** increases when [CO] decreases, i.e., the transient flash photolysis signal at 510 nm under Ar is greater than that under CO. A similar decrease in the magnitude of the transient signal at 510 nm was also observed in the presence of phosphorus ligands (vide infra).

Caspar and Meyer reported that the decay rate of **2** under Ar is sensitive to the probe beam intensity,[2a] i.e., a more intense probe beam accelerates the reaction **2** → **1**. They also indicated that rate is no longer sensitive to beam intensity when the reaction is carried out under CO. Our experiments confirmed the latter observation. However, we found that the quantity of **2** produced after the flash decreases when probe beam intensity is reduced, whereas the amount of **7** formed and its rate of decay are insensitive to beam intensity (Figure 5).

These observations provide additional evidence as to how **2** and **7** are produced. Concerted CO loss and structural rearrangement

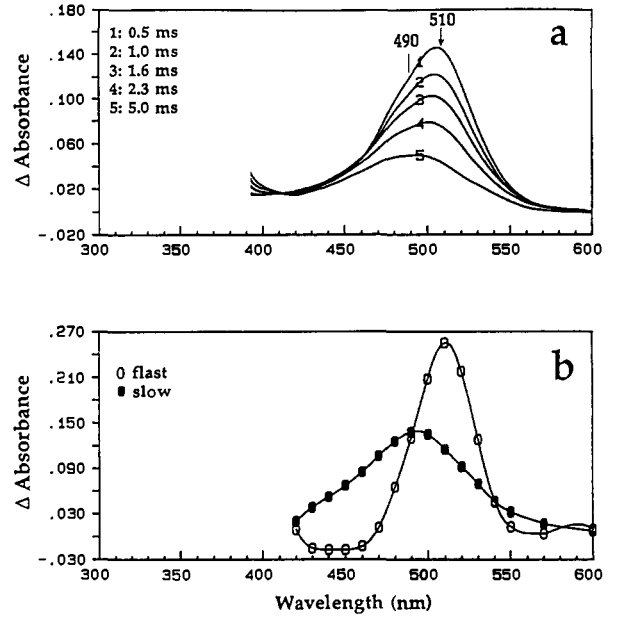

Figure 6. Time-resolved visible spectra of $Cp_2Fe_2(CO)_4$ in hexane under 1 atm of CO. (a) Obtained using laser flash photolysis with photodiode array detection. (d) Obtained using conventional flash photolysis.

from *trans*-**1** upon photoexcitation is unlikely to be the only mechanism for formation of **2**.[1c] A precursor with a considerably longer lifetime than the usual excited-state molecule, but which is still short-lived, seems to exist.[4g] Poliakoff, Turner, and coworkers have reached a similar conclusion via a different approach using time-resolved IR spectroscopy.[4g] Species **6**, a structural isomer of **2**, may contribute in part to the increased yield of **2** under increased probe beam irradiation. However, the relatively low yield of **6** even in the absence of visible irradiation (Figure 1) following the flash photolysis and its long lifetime rule it out as the major precursor to **2**. These points are further discussed in section G.

Time-resolved UV–visible spectra regarding **2** and **7** were also obtained using laser flash photolysis with photodiode array detection[14] (Figure 6a) or conventional flash photolysis (Figure 6b). Figure 6a shows the spectra following N_2 laser photolysis (337 nm) at various delay times (0.5–5.0 ms). Two band features are seen in the spectra: a stronger band at 510 nm disappears rapidly over this time scale while the weaker band centered at ~490 nm is more evident at the longer delay time. Spectra obtained using conventional flash photolysis enabled us to resolve the two bands corresponding to **2** (fast) and **7** (slow), respectively (Figure 6b).

Using laser flash photolysis, we also examined the kinetics of the photochemical reaction of **1** under CO. Immediately after

(18) *Carbon Monoxide*; Cargill, R. W., Ed.; Solubility Data Series; Pergamon Press: New York, 1990; pp 51–52.

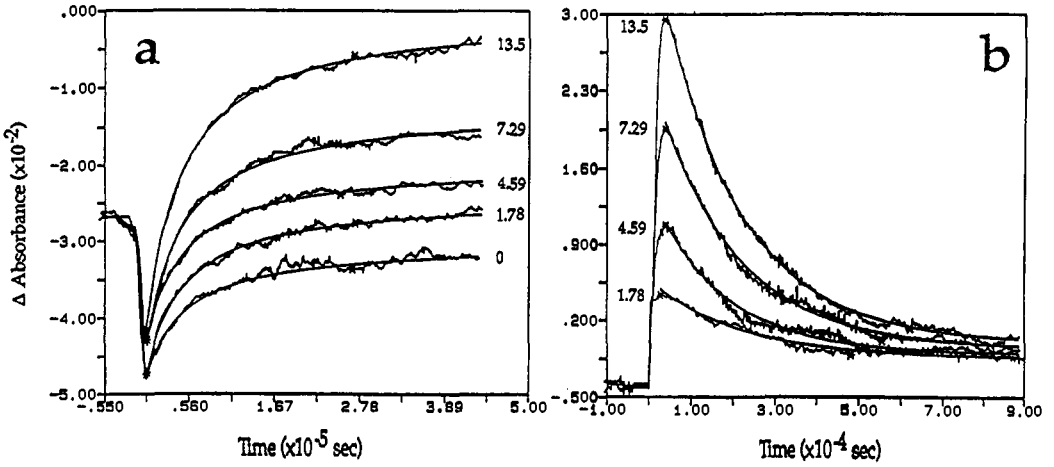

Figure 7. Transient signals after laser flash photolysis of $Cp_2Fe_2(CO)_4$ in hexane under various CO partial pressures. The calculated CO concentrations (in mM) are labeled at the end or beginning of the traces. (a) The signals at 430 nm on a 50-μs time scale represent recovery of absorbance due to radical recombination and a second process leading to **8**. The solid lines are fits to a second-order rate law. (b) Transient signals at 400 nm on a 1-ms time scale represent decay of the absorbance due to **8**. The solid lines are fits to a first-order rate law.

the flash, bleaching of the weak band at 430 nm due to **1** (Figure 2a) is observed. Under Ar ([CO] = 0 in Figure 7a), partial recovery of the bleaching in the 50-μs time domain can be attributed to the recombination of the radicals **3** to form **1**, which is consistent with what has been previously reported.[2a] However, under increased [CO], the absorbance eventually exceeds the preflash level to reach different values dependending on [CO]. Nevertheless, the rate of recovery is approximately independent of [CO] and can be fitted reasonably well to a second-order process. These observations, demonstrated in Figure 7a, provided the initial evidence for formation of yet another species, designated **8**.

8 is distinguished from the other transient intermediates **2**, **3**, **6**, and **7** because it decays at a different rate. Figure 7b shows the decay signals at 400 nm corresponding to various [CO]. The transient absorptions shown here represent decay of the species which is formed along with **1** in the shorter time domain, as shown in Figure 7a. The decay process obeys first-order kinetics with the rate constant being independent of [CO] ($k \approx 5 \times 10^3$ s^{-1} at 22 °C). From Figure 7, it is evident that the amount of **8** formed increases with [CO]. There is at this point no clear evidence as to the identity of its decay product (however, vide infra). Due to the probe beam wavelength limitation (380–700 nm) on the laser photolysis system, we were unable to identify λ_{max} for **8**, other than that $\lambda_{max} < 400$ nm. Using time-resolved infrared spectroscopy, Moore et al. have also observed an intermediate, designated X, in a solution of **1** in cyclohexane under 1 atm of CO.[4a] X appears 25 μs after the flash and decays with $k \approx 4.6 \times 10^3$ s^{-1}. The kinetic behavior of X fits very well with species **8** observed in our experiments.

C. Flash Photolysis of 1 under CO at Low Temperatures. At −180 °C in MCH–3MP (9:1), formation of only **2** was observed after flash photolysis when the IR cell was loaded with a solution of **1** under 1 atm of either Ar or CO. Photolysis in the −180 to −100 °C temperature range afforded similar results. At −70 °C under CO, after a single flash we obtained the difference IR spectra shown in Figure 8a. The three negative bands are due to loss of **1**. Bands of **2** and **6** have disappeared due to their reaction with CO. Analysis of the spectra indicates that the new peaks belong to two groups. One group (2040, 1992, 1974, 1967, and 1941 cm^{-1}, vide infra) decreases with $t_{1/2} \approx 30$ min, with the concurrent growth of the other group (1990, 1956, 1941, and 1684 cm^{-1}). The difference IR spectra taken after flash irradiation of a solution under CO at −25 °C, shown in Figure 8b, demonstrate clearly that the second group of bands, belonging to a single species, disappear at the same rate to form **1** at this temperature. It should be pointed out that the IR bands in Figure 8 were also observed, albeit with much weaker absorbances, together with those of **2** and **6**, when the flash photolysis was carried out under Ar.

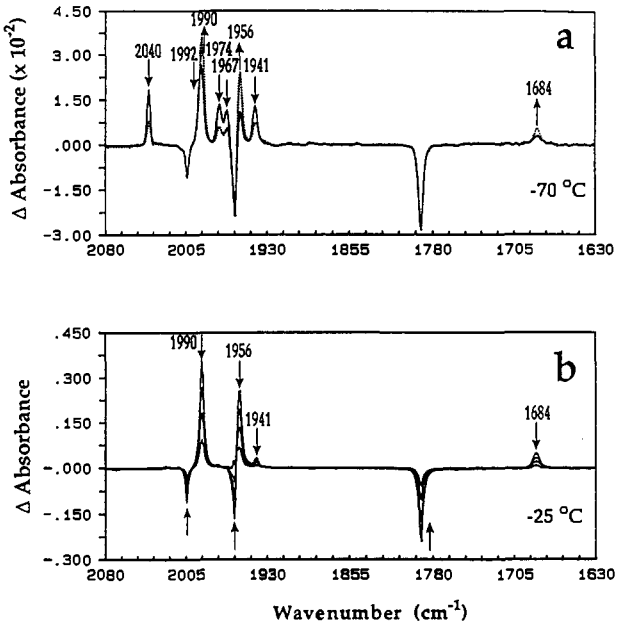

Figure 8. Difference IR spectra of $Cp_2Fe_2(CO)_4$ in MCH–3MP (9:1) saturated with 1 atm of CO in a 1-mm CaF_2 cell. (a) Before and after one flash at −70 °C; (—) 1 min after the flash, (···) 36 min after the flash. (b) Before and after (1, 40, 80, and 150 min, respectively) seven flashes at −25 °C.

The experiments that afforded the IR spectra of Figure 8 were repeated using UV–visible detection. The interconversion of two species at −70 °C, λ_{max} = 392 and 484 nm, respectively, is clearly seen, with a well-defined isosbestic point (Figure 9a). Consistent with the IR experiment (Figure 8a), it shows that no recovery of **1** (λ_{max} = 350 nm) is noticeable at −70 °C in this time domain. Figure 9b parallels Figure 8b in that the species with λ_{max} = 488 nm decays to form **1**.

Recalling the new species discussed in the previous section and combining the spectroscopic data obtained in Figures 8 and 9 with those in flash photolysis at room temperature, we can assign IR bands (ν_{CO}) 1990, 1956, 1941, and 1684 cm^{-1} to **7** and 2040, 1992, 1974, 1967, and 1941 cm^{-1} to **8**. It appears that **8** mainly converts to **7** instead of forming **1** directly. The spectroscopic data for relevant species observed are summarized in Table I.

Experiments involving the use of highly enriched ^{13}CO were also carried out. The fully exchanged complex $Cp_2Fe_2(^{13}CO)_4$ (**1***) was prepared from **1** and ^{13}CO. The difference IR spectra shown in Figure 10 were taken after one flash at −70 °C for various combinations of the starting complex (**1** or **1***) and cover

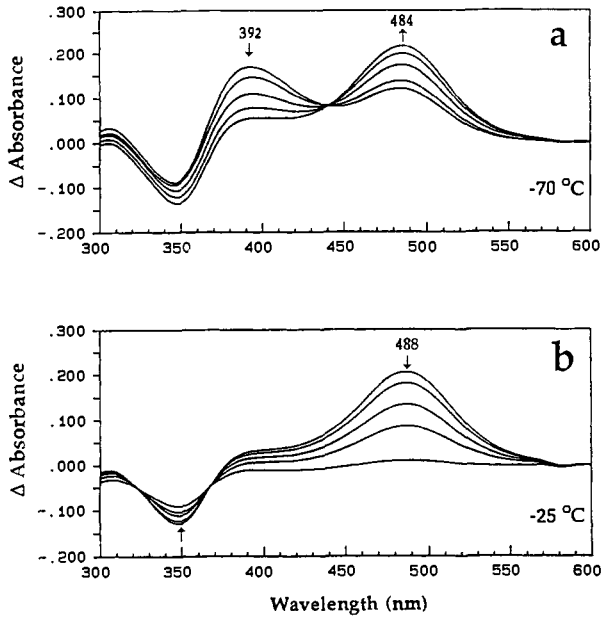

Figure 9. Difference UV–visible spectra of $Cp_2Fe_2(CO)_4$ in MCH–3MP (9:1) saturated with 1 atm of CO in a 1-mm CaF_2 cell. (a) Before and after seven flashes at −70 °C. The successive spectra represent 1, 5, 15, 30, and 50 min following the flashes. (b) The successive spectra represent 2, 15, 45, 90, and 150 min after the solution is warmed to −25 °C.

Table I. Spectroscopic Data for Species Observed in Photolysis of **1**

species	IR (relative intensity) ν_{CO}, cm^{-1}	UV–visible λ_{max}, nm	solvent/ T (°C)
1	2006(1.0), 1961(2.1), 1794(2.1)	350 (s), 430 (w), 530 (w)	hexane/25
2	1823[a]	510 (s)	cyclohexane/25
	1819		MCH–3MP/-25
	1812		MCH–3MP/-180
3	2004(1.0),[a] 1940(1.0)[a]		cyclohexane/25
6	1839(2.3), 1786(1.5), 1674(1.0)	~380	hexane/25
7	1990(10.8), 1956(9.3), 1941(1.0), 1684(1.3)	484	MCH–3MP/-70
		488	MCH–3MP/-25
		490	hexane/25
8	2040(1.5), 1992(1.2), 1974(1.1), 1967(1.0), 1941(1.0)	392	MCH–3MP/-70

[a] Reference 4a.

gas (^{12}CO or ^{13}CO). The results indicate that essentially *all* the CO groups in **8** and **7** were exchanged. One can see clearly that {**1** + ^{12}CO} (Figure 10a) and {**1*** + ^{12}CO} (Figure 10b) generated almost the same IR bands, as did {**1** + ^{13}CO} (Figure 10c) and {**1*** + ^{13}CO} (Figure 10d). The label of the cover gas largely determines the labeling of CO groups in **8** and **7**. The spectra in Figure 10d represent ^{13}CO-exchanged **8** and **7**, i.e., **8*** and **7***, respectively, keeping in mind that the spectra are complicated by the existence of ~18% of ^{18}O in the ^{13}CO used.

The peaks marked P in Figures 10b and c are ascribed to the partially exchanged products $Cp_2Fe_2(^{13}CO)_{4-n}(^{12}CO)_n$ (n = 1, 2, 3). These peaks were confirmed by separately preparing a solution which contained partially exchanged dimers. Figure 11a shows the IR spectra of $Cp_2Fe_2(^{13}CO)_{4-n}(^{12}CO)_n$ (n = 0, 1, 2, 3), in which the peaks due to **1** (n = 4) have been removed for clarity.

D. Structures and Formation of 7 and 8. Both **7** and **8** are formed more extensively under CO. Their formation is thus inconsistent with their descent from a CO-loss product. **8** apparently has five terminal CO groups. The grouping of IR bands is consistent with the presence of three CO groups on one Fe atom

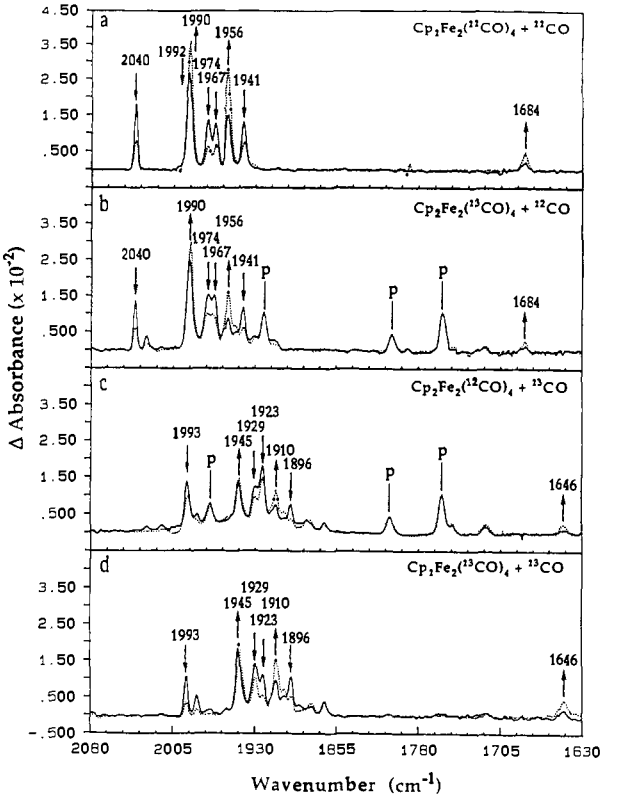

Figure 10. Difference IR spectra of $Cp_2Fe_2(^{12}CO)_4$ or $Cp_2Fe_2(^{13}CO)_4$ in MCH–3MP (9:1) saturated with 1 atm of ^{12}CO or ^{13}CO, before and after one flash at −70 °C. The negative peaks due to the starting material have been removed for clarity.

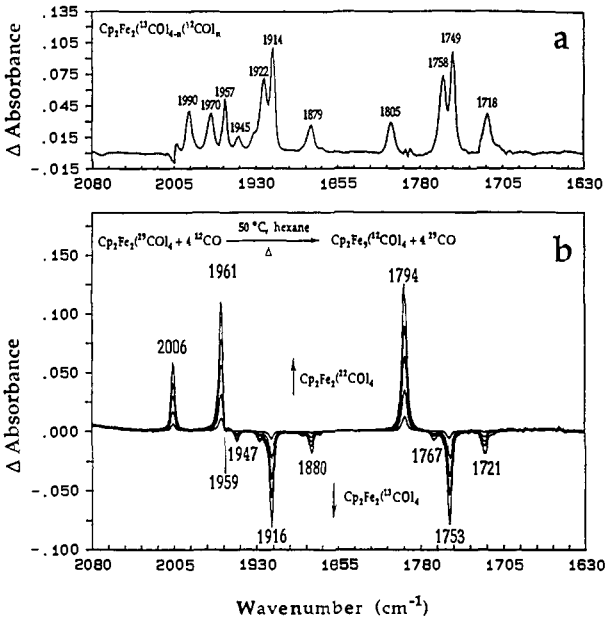

Figure 11. (a) IR spectra of $Cp_2Fe_2(^{13}CO)_{4-n}(^{12}CO)_n$ (n = 0, 1, 2, 3) in MCH–3MP (9:1) at −70 °C. (b) The IR spectral changes during the thermal exchange reaction of $Cp_2Fe_2(^{13}CO)_4$ with ^{12}CO in hexane at 50 °C. The successive spectra represent the difference between before and 60, 180, 340, 490, and 730 min after the solution is exposed to ^{12}CO. The band at 1959 cm^{-1} for $Cp_2Fe_2(^{13}CO)_4$, not seen here due to overlap, is seen in the spectrum of pure $Cp_2Fe_2(^{13}CO)_4$.

and two CO groups on the second Fe. For example, IR bands at 2047, 1980, and 1972 cm^{-1} are observed in $(\eta^4\text{-}C_5H_6)Fe(CO)_3$[19] and at 1992 and 1941 cm^{-1} in $CpFe(CO)_2SiEt_3$.[20] The band at

(19) Blaha, J. P.; Wrighton, M. S. *J. Am. Chem. Soc.* **1985**, *107*, 2694.

1684 cm^{-1} for **7** is most likely due to the presence of a semibridging CO or an acyl-like group in the molecule.

In their most recent report,[4g] Poliakoff, Turner, and co-workers have identified two CO bands at 1977 and 1942 cm^{-1} for the species which is consistent with **8** in our experiments (vide supra). A similar observation was made in CO matrices at 20 K.[21] They have discussed two possible structures for this species: $Cp(CO)_3Fe$ formed by reaction of $Cp(CO)_2Fe$ with CO and the unbridged isomer of $[Cp(CO)_2Fe]_2$ (non-**1**). However, no evidence for reaction of $Cp(CO)_2Fe$ with CO was observed in their experiments; further, it is not clear why the presence of CO should promote the formation of an unbridged isomer. Failure to observe the additional bands of **8** in their time-resolved IR experiments may be also a result of limited spectral resolution and sensitivity, a situation similar to that which occured in recognition of **6** (vide supra).

The extensive CO exchange, even in the course of a single flash, in the experiments using isotopically labeled CO, strongly suggests that formation of **8** and **7** occurs via a radical pathway; the lability of 17-electron $Cp(CO)_2Fe$ radicals is well-established.[4f,22] The most plausible explanation for the formation of **8** and **7** is that a $Cp(CO)_2Fe^{\bullet}$ radical reacts with CO to form a nominally 19-electron species ($Cp(CO)_3Fe$),[19] which then combines with $Cp(CO)_2Fe^{\bullet}$ to form **8**, which in turn decays to form **7**.

The facile CO exchange on the 17-electron radical is further supported by thermal exchange experiments. A solution of $Cp_2Fe_2(^{13}CO)_4$ in hexane under 1 atm of ^{12}CO was stirred at 50 °C in the dark. Progress of the reaction was monitored using IR spectra of samples withdrawn from the reaction solution. The results are shown in Figure 11b. Clearly, at any stage of the reaction, the fully exchanged complex $Cp_2Fe_2(^{12}CO)_4$ was observed as the only product without intermediacy of any partially exchanged dimer. The explanation is that the thermal exchange occurs exclusively via homolysis of the Fe–Fe bond; the rate of CO exchange on the carbonyl radical is much faster than the radical recombination. The rate constant for $P(OMe)_3$ substitution of CO in $Cp(CO)_2Fe$ to form $Cp(CO)FeP(OMe)_3$, 9×10^8 M^{-1} s^{-1},[4f] is very close to that for recombination of two $Cp(CO)_2Fe^{\bullet}$ radicals, 3×10^9 M^{-1} s^{-1}.[2a] The rate constant for CO exchange is likely similar to that for $P(OMe)_3$ substitution on $Cp(CO)_2Fe^{\bullet}$. Since the concentration of CO from the cover gas is much higher than the radical concentration, it is not surprising that all carbonyls in the radical are exchanged before they recombine to form the dimer. The rate constant for growth of **1** based on the spectra shown in Figure 11b, $(8.1 \pm 0.2) \times 10^{-6}$ s^{-1} at 50 °C, should equal that for the rate-determining step, i.e., homolysis of the Fe–Fe bond. In fact, our rate constant is consistent with that obtained by both Rosenblum[23] and Tyler[3d] using indirect methods. The thermal exchange experiment provides a convenient alternative method for determining rate constants for such homolysis processes in similar dinuclear carbonyls.

The evidence for reaction of the formally 19-electron species $Cp(CO)_3Fe$ with $Cp(CO)_2Fe$ to afford **8** implies that the two species are in fast equilibrium in the presence of CO, although $Cp(CO)_3Fe$ may be present in smaller concentration than $Cp(CO)_2Fe$. The low relative concentration of $Cp(CO)_3Fe$ should preclude its reaction with another $Cp(CO)_3Fe$. Assuming a rate constant of 1×10^9 M^{-1} s^{-1} for reaction of $Cp(CO)_2Fe$ with CO to form $Cp(CO)_3Fe$, the time for establishing an equilibrium between $Cp(CO)_3Fe$ and $Cp(CO)_2Fe$ is very short, $t_{1/2} < 70$ ns under 1 atm of CO. Thus, it is not surprising that such a process could not be observed in the reported time-resolved IR experiments by Poliakoff, Turner, and co-workers,[4g] since the fastest rise time in their detection system is 125 ns. Nevertheless, the presence of $Cp(CO)_3Fe$ and its reaction with $Cp(CO)_2Fe$ to form **8** are expected be be observable using their detection system. In fact, the earlier report indicated that **8** appears 25 μs after the flash,[4a] which is a reasonable time scale for reaction of $Cp(CO)_3Fe$ and $Cp(CO)_2Fe$. Scheme II shows the possible reaction steps involved in the aforementioned reactions, where *CO designates CO from the cover gas.

Scheme II

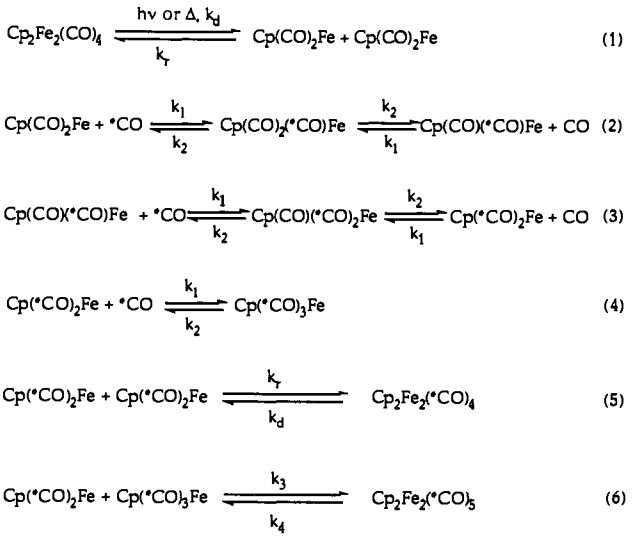

It is noteworthy that **8** and **7** are also observed when a solution of **1** is photolyzed under Ar at low temperatures (−100 to −25 °C), although they are produced in much smaller amounts compared to the reaction under CO.[13] Given the very low concentration of free CO formed as a result of CO loss, reactions 4 and 6 (where CO* = CO) are unlikely to account for the formation of $Cp(CO)_3Fe$ and **8**. We thus postulate the formation of $Cp(CO)_3Fe$ and Cp(CO)Fe radicals directly from **1** as minor photoproducts via an unsymmetrical fragmentation (eq 7), in addition to $Cp(CO)_2Fe$ formed via symmetrical cleavage (eq 8). According

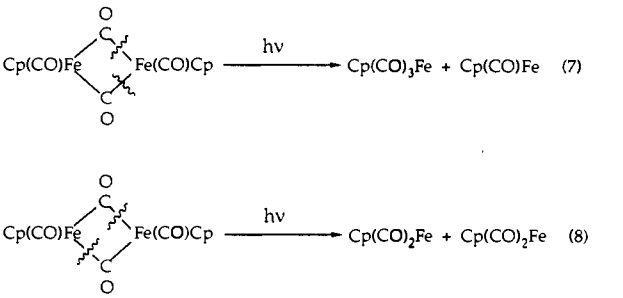

to neutron diffraction experiments[24] and molecular orbital calculations,[25] there is no buildup of electron density along the Fe–Fe axis; two Fe centers are bridged together through two CO groups. The two pathways differ only in the choices of cleavage of the (O)C–Fe bonds.

Failure to observe **8** and **7** at lower temperatures (< −100 °C) is probably due to a strong cage effect, i.e., radicals derived from **1** rapidly recombine before undergoing subsequent reactions described in eqs 4 and 6 (where CO* = CO).

The IR spectrum of **8** is equally consistent with two structures. The first one could arise if **3** attacks the Cp ring of $Cp(CO)_3Fe$ to yield **8a**. The second structure results from formation of an Fe–Fe bond (**8b**).

Structure **8a** is supported by the findings of Blaha and Wrighton, who observed formation of (η^4-C_5H_5(*exo*-$CH_2C_6H_5$))$Fe(CO)_3$ upon near-UV irradiation of (η^5-C_5H_5)Fe-$(CO)_2(CH_2C_6H_5)$ under 2 atm of CO.[19] Attack of the $^{\bullet}CH_2C_6H_5$

(20) Pannell, K. H.; Wu, C. C.; Long, G. J. *J. Organomet. Chem.* **1980**, *186*, 85.
(21) Ref 4g, note 51.
(22) (a) Therien, M. J.; Trogler, W. C. *J. Am. Chem. Soc.* **1987**, *109*, 5127. (b) Trogler, W. C. In *Organometallic Radical Processes*; Trogler, W. C., Ed.; Elsevier: Amsterdam, 1990; p 306.
(23) Cutler, A. R.; Rosenblum, M. *J. Organomet. Chem.* **1976**, *120*, 87.
(24) Mitschler, A. M.; Rees, B.; Lehmann, M. S. *J. Am. Chem. Soc.* **1978**, *100*, 3390.
(25) Benard, M. *Inorg. Chem.* **1979**, *18*, 2782.

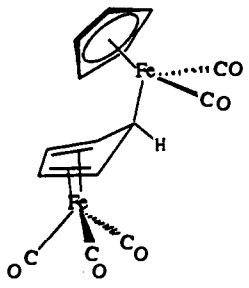

8a

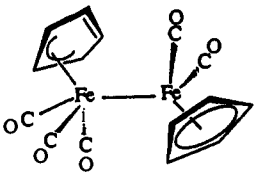

8b

radical on the Cp ring was interpreted in terms of a considerable delocalization of unpaired electron spin to the Cp ring to give a more stable 18-electron configuration at Fe. Analysis of the UV–visible spectra, however, supports structure **8b**. The existence of a band at 392 nm is consistent with a structure involving a nonbridging Fe–Fe bond. For example, a very intense band at 398 nm for $Cp(CO)_3Mo\text{-}Fe(CO)_2Cp$ is ascribed to the $\sigma_b \rightarrow \sigma^*$ transition.[26] Furthermore, the UV–visible spectra for some known complexes, e.g., $(\eta^4\text{-}C_5H_5(CH_2C_6H_5))Fe(CO)_3$[19] and $(\eta^5\text{-}Cp)(CO)_2Fe(\eta^1\text{-}Cp)$,[27] which closely resemble the two fragments of **8a**, all exhibit absorbance at relatively shorter wavelength (λ_{max} < 350 nm). It has been indicated that the coupling chemistry does not necessarily reflect the distribution of unpaired spin density on the radical, which can be very different in the transition and ground states.[28] We therefore consider **8b** as the more likely structure.

Several possibilities suggest themselves for the structure of **7**. Among them, **7a** has a semibridging CO and two terminal CO groups on each Fe atom. **7b** has a structure analogous to that proposed by Tyler, Schmidt, and Gray (**5**) for a species observed when **1** is photolyzed with $P(O\text{-}i\text{-}Pr)_3$ at low temperatures.[3a,b] Rearrangement of a carbonyl group in **8b** to form **7a** or **7b** seems to be a plausible mechanism for the observed conversion. However, considering its unsymmetrical structure, one could expect a total of five CO stretching bands for **7a** instead of four as observed. The band pattern of a complex which resembles **7b** in structure $(Cp(CO)_2Re(\mu\text{-}CO)Re(CO)_2Cp$, **9**), 1992(0.7), 1956(10.0), 1923(9.0), 1904(1.2), and 1740(4.5) cm^{-1} (in cyclohexane, relative intensity on a transmittance scale in parentheses),[29] is closely similar to **7** (Table I). Assuming that the highest ν_{CO} band is too weak to be seen in **7**, the other terminal ν_{CO} frequencies shift to higher values (33–36 cm^{-1}) in **7** compared to **9**. The bridging ν_{CO} frequency in **7** is 56 cm^{-1} lower than in **9**. However, there is a Re–Re bond in **9** and no Fe–Fe bond in **7b**. This difference could account for the stretching frequencies of bridging CO in **7b** shifting to smaller value, since a typical acyl group in iron carbonyls, $Cp(CO)_2Fe\text{-}COR$, exhibits ν_{CO} lower than 1700 cm^{-1}.

Another possible structure (**7c**) could arise from **8** by loss of a CO from the $(\eta^3\text{-}Cp)(CO)_3Fe$ half of **8b** with formation of a semibridge. This structure would be consistent with the observation of only four bands for **7**. Furthermore, the existence of a semibridging CO in **7** is also consistent with the visible band observed at 490 nm (Table I). For example, loss of a CO from $(CO)_5Mn\text{-}Mn(CO)_5$ produces $(CO)_4Mn(\mu\text{-}\eta^1,\eta^2\text{-}CO)Mn(CO)_4$. This molecule, which contains a Mn–Mn bond and a semibridging CO, exhibits λ_{max} at 480–500 nm.[30] Attempts to obtain more structural information on **7** by analyzing the IR spectra of ^{13}CO-exchanged species (**7***, Figure 10d) were not successful due to the obscured features of the weaker bands. At this stage of our understanding, **7c** appears to be the more plausible structure, but we cannot rule out **7b**.

Table II. Rate Constants and Activation Parameters

reaction	rate constant (25 °C)	ΔH^*(kcal mol^{-1})	ΔS^* (eu)
2 + CO → 1	5.7×10^4 M^{-1} s^{-1}	7.6 ± 0.2	−11.5 ± 0.8
8 → 7 + CO	5.4×10^3 s^{-1}	19.8 ± 0.5	25.4 ± 2.0
7 → 1	6.2×10^1 s^{-1}	22.3 ± 0.4	24.3 ± 1.3
6 + CO → 1	≈3 M^{-1} s^{-1} [a]		

[a] Calculated by assuming $[CO]_0 \approx 6 \times 10^{-5}$ M, which can be estimated from the bleaching of **1** after flash photolysis in Figure 1.

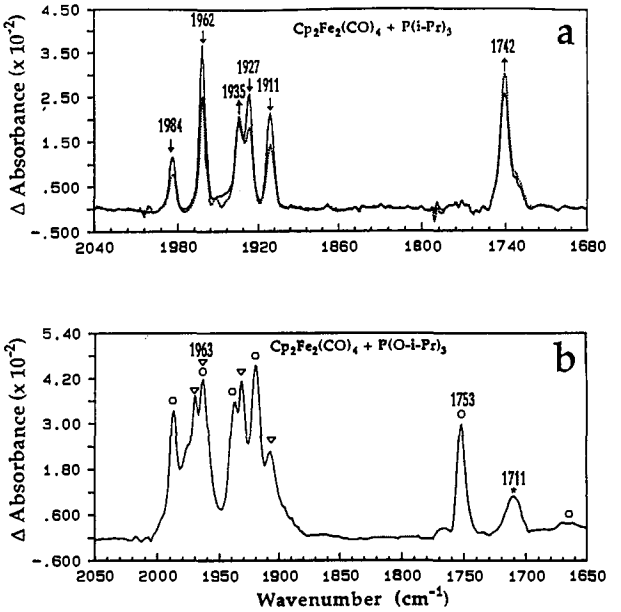

Figure 12. (a) Difference IR spectra of a 3MP solution of $Cp_2Fe_2(^{12}CO)_4$ (0.5 mM) and $P(i\text{-}Pr)_3$ (20 mM) before and after one flash at −70 °C. (—) 1 min after the flash, (···) 50 min after the flash. (b) The difference IR spectra of a 3MP solution of $Cp_2Fe_2(^{12}CO)_4$ (0.5 mM) and $P(O\text{-}i\text{-}Pr)_3$ (30 mM) before and after seven flashes at −70 °C. Bands labeled O are due to $Cp_2Fe_2(CO)_3P(O\text{-}i\text{-}Pr)_3$. The band * is assigned to $[Cp(CO)FeP(O\text{-}i\text{-}Pr)_3]_2$. Bands labeled □ and ▽ are attributed to two other unidentified species.

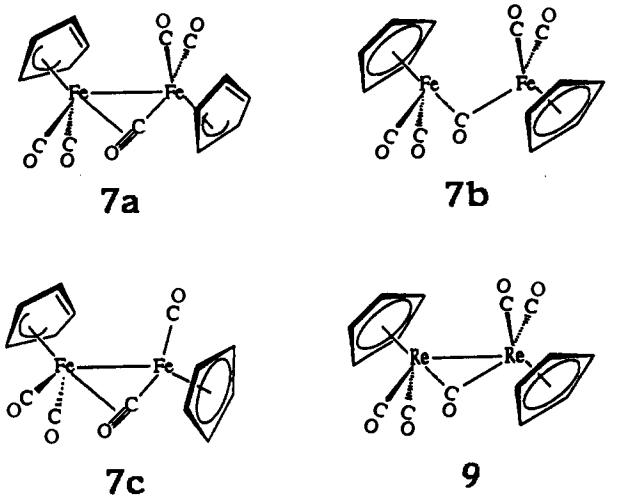

7a 7b 7c 9

E. Reactions of Observed Intermediates. Reactions of **2** with CO and other nucleophiles have been reported elsewhere in detail.[12] We note that **8** decays faster than **2** at room temperature under CO while the reverse order occurs at −70 °C. This result implies that reaction of **8** has a relatively higher activation energy. Rate constants for reactions of **2**, **8**, and **7** at various temperatures have been determined, and the activation parameters together with the

(26) Abrahamson, H.; Wrighton, M. S. *Inorg. Chem.* **1978**, *17*, 1003.
(27) Piper, T. S.; Wilkinson, G. *J. Inorg. Nucl. Chem.* **1956**, *3*, 104.
(28) (a) Hamon, J.-R.; Astruc, D.; Michaud, P. *J. Am. Chem. Soc.* **1981**, *103*, 758. (b) Astruc, D. *Acc. Chem. Res.* **1986**, *19*, 377. (c) Astruc, D. *Chem. Rev.* **1988**, *88*, 1189.
(29) Foust, A. S.; Hoyano, J. K.; Graham, W. A. G. *J. Organomet. Chem.* **1971**, *32*, C65.
(30) (a) Yesaka, H.; Kobayashi, T.; Yasufuku, K.; Nagakura, S. *J. Am. Chem. Soc.* **1983**, *105*, 6249. (b) Church, S. P.; Hermann, H.; Grevels, F.-W.; Schaffner, K. *J. Chem. Soc., Chem. Commun.* **1984**, 785. (c) Zhang, H.-T.; Brown, T. L. *J. Am. Chem. Soc.* **1993**, *115*, 107.

Scheme III

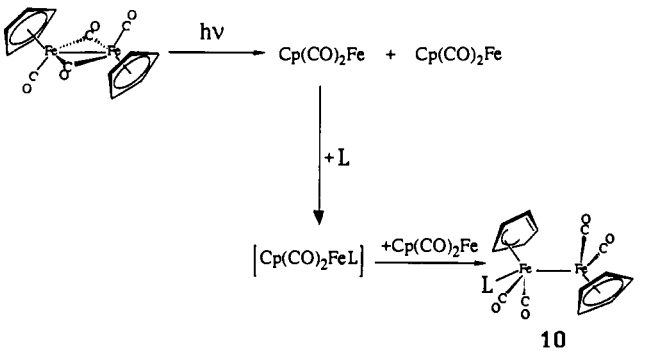

10

rate constant data at 25 °C are listed in Table II. The very positive entropy of activation for transformation from **8** to **7** is consistent with the proposed intermediate and mechanism, i.e., loss of CO from the crowded $(\eta^3\text{-Cp})(CO)_3Fe$ half of **8** is entropically favored. Conversion of **7** to **1** has relatively high activation enthalpy and entropy. This might imply that the cleavage of the semibridging CO to form the nonbridging intermediate (non-**1**) is a rate-determining step.

F. Flash Photolysis of 1 in the Presence of Phosphorus Ligands at Low Temperature. A single flash photolysis of **1** in the presence of $P(i\text{-Pr})_3$ at −70 °C in 3MP afforded the spectra in Figure 12a, where the negative peaks due to **1** have been removed. Bands at 1935 and 1742 cm^{-1} are ascribed to the monosubstituted dimer $Cp_2Fe_2(CO)_3P(i\text{-Pr})_3$. The other four bands at 1984, 1962, 1927, and 1911 cm^{-1} are consistent with a species which has a structure analogous to **8b**, with one CO group in the $(\eta^3\text{-Cp})(CO)_3Fe$ half being replaced by $P(i\text{-Pr})_3$, $(\eta^5\text{-Cp})(CO)_2Fe\text{-}Fe(CO)_2(\eta^3\text{-Cp})P(i\text{-Pr})_3$ (**10**). The corresponding UV–visible spectrum shows a

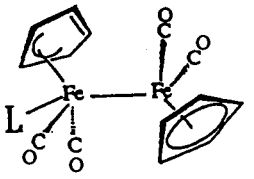

10

band at 410 nm for this species, shifted to a longer wavelength compared to **8**. At higher temperatures, **10** apparently decomposes to form **1** or $Cp_2Fe_2(CO)_3P(i\text{-Pr})_3$. An intermediate analogous to **7** or **5**, containing a bridging CO, was not observed in the −70 to 25 °C temperature range. A plausible explanation for formation of **10** is as described in Scheme III, i.e., via a radical mechanism.

Flash photolysis of **1** with $P(O\text{-}i\text{-Pr})_3$ in 3MP at −70 °C led to a difference IR spectrum from a single flash, as shown in Figure 12b. Besides the monosubstituted product $Cp_2Fe_2(CO)_3P(O\text{-}i\text{-Pr})_3$ (labeled O, strong band at 1753 cm^{-1}), we observed at least three more species on the basis of the evolution of the IR and UV–visible spectra after flash photolysis. A species (**5**) observed by Tyler et al.[3a,b] was reported to exhibit ν_{CO} at 1720 cm^{-1} in THF at −78 °C; no IR data for the terminal CO region were reported. In our experiment, however, we observed a band at 1711 cm^{-1} (Figure 12b). The band at 1711 cm^{-1} is most likely due to the disubstituted product $[Cp(CO)FeP(O\text{-}i\text{-Pr})_3]_2$ on the basis of the comparison with $[Cp(CO)FeP(OMe)_3]_2$. It is possible that the differences in solvent (THF, ethyl chloride vs 3MP) and photolysis conditions (continuous vs flash) are responsible for the different observations. However, using time-resolved IR spectroscopy at room temperature in cyclohexane, Poliakoff, Turner, and co-workers observed a band at 1720 cm^{-1}, which they unequivocally attributed to $[Cp(CO)FeP(O\text{-}i\text{-Pr})_3]_2$ instead of to **5** as suggested by Tyler et al. If, in fact, the same species has been observed in all three studies (ν_{CO} = 1720 cm^{-1} in THF at −78 °C;[3a,b] 1711 cm^{-1} in 3MP at −70 °C; 1720 cm^{-1} in cyclohexane at 25 °C[4g]), then the various ν_{CO} values may arise from solvent and temperature effects as well as uncertainties in determination of band positions.

Low-temperature flash photolysis of **1** in the presence of $P(OMe)_3$ afforded spectral features similar to $P(O\text{-}i\text{-Pr})_3$. Warmup of the solution of **1** + L (L = $P(i\text{-Pr})_3$, $P(O\text{-}i\text{-Pr})_3$, $P(OMe)_3$) resulted in the disappearance of bands other than those due to $Cp_2Fe_2(CO)_3L$ (L = $P(i\text{-Pr})_3$, $P(O\text{-}i\text{-Pr})_3$, $P(OMe)_3$) and $[Cp(CO)FeL]_2$ (L = $P(OMe)_3$). We have found that $[Cp(CO)FeP(OMe)_3]_2$ is not very stable at room temperature in solution; it undergoes a reaction involving Fe–Fe bond homolysis.[12] It is not surprising that $[Cp(CO)FeP(O\text{-}i\text{-Pr})_3]_2$ is more labile in respect to Fe–Fe bond homolysis, so it decomposes at lower temperatures. Direct flash photolyses at room temperature also produced the same final products.

No net photoreaction was observed when $P(C_6F_5)_3$ was photolyzed with **1** at room temperature. However, at −70 °C in 3MP following flash photolysis we observed transient species **8** and **7** and also another intermediate (**11**). The latter exhibits IR bands at 1958, 1809, and 1765 cm^{-1} which disappear when the solution is warmed to room temperature. A possible composition for **11** is $Cp_2Fe_2(CO)_3P(C_6F_5)_3$. The fact that **8** and **7** are still observed implies that reaction of $P(C_6F_5)_3$ with the $Cp(CO)_2Fe$ radical is negligible.

G. Mechanism for Formation of 2. We were surprised to note that the presence of CO or a phosphorus ligand reduced the initial transient signal (510 nm) due to $Cp_2Fe_2(\mu\text{-}CO)_3$, in comparison with reaction under Ar. Though $P(C_6F_5)_3$ is relatively unreactive toward $Cp_2Fe_2(\mu\text{-}CO)_3$,[12] the amount of **2** formed initially after the flash, on the basis of the absorbance change, is at most only about 60% of that under Ar in the absence of ligand. Furthermore, the amount of **2** initially observed after flash photolysis is also sensitive to probe beam intensity (section B). It has also been noted that in the presence of THF, the amount of $Cp_2Fe_2(\mu\text{-}CO)_3$ produced is suppressed.[4c,g] The result was originally attributed to a variation in solvent polarity, which affects the relative distribution of cis and trans isomers.[4c] It is unlikely, however, that the presence of L in low concentration should change the medium polarity greatly. Most recently, Poliakoff, Turner, and co-workers have reported new evidence which supports the existence of a precursor to $Cp_2Fe_2(\mu\text{-}CO)_3$.[4g] According to these authors, the so-far unidentified precursor is very short lived (<125 ns).[4g]

An unsaturated CO-loss species (I) has been suggested as a possible precursor to $Cp_2Fe_2(\mu\text{-}CO)_3$.[4g] Photolysis of $Cp_2Fe_2(CO)_4$ creates I via loss of a terminal CO. I then isomerizes to

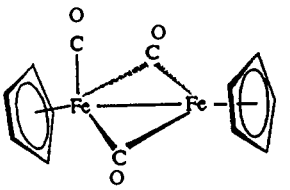

I

$Cp_2Fe_2(\mu\text{-}CO)_3$ or reacts with a nucleophile to form the monosubstituted product $Cp_2Fe_2(CO)_3L$. The existence of I is consistent with the observation that $Cp_2Fe_2(\mu\text{-}CO)_3$ and $Cp_2Fe_2(CO)_3$ THF share a common precursor.[4g]

Another possible structure for the short-lived precursor is **4** (Scheme I), originally proposed by Tyler et al. to be an intermediate responsible for the formation of the monosubstituted product $Cp_2Fe_2(CO)_3L$ via **5** (Scheme I).[3a,b] It is not unreasonable to propose that **4** is also responsible for formation of **2**. In the presence of a nucleophile, the unimolecular processes leading to **2** compete with a bimolecular reaction with the nucleophile to yield the substituted product. It is interesting to note that structure **4** and **7c** differ in the type of CO bridge, i.e., symmetric bridge in **4** vs semibridge in **7c**, which could be responsible for the difference in their reactivities and lifetimes. Similarly, **6** is more stable than **2**. Nominally, structures **7c** and **6** are saturated, whereas **4** and **2** are unsaturated species if the iron centers are considered to be saturated when 18 valence shell electrons are

counted on each metal center without introducing a multiple Fe–Fe bond.

To understand the effect of probe beam irradiation (visible) on the production of $Cp_2Fe_2(\mu\text{-}CO)_3$, one can envision a light-induced transformation of the precursor (e.g., I or **4**) to **2**. The precursor presumably can react with THF or other nucleophiles, thus suppressing formation of $Cp_2Fe_2(\mu\text{-}CO)_3$. Reaction of the precursor with a nucleophile should be very rapid. Poliakoff and Turner et al. have estimated that the rate constant for formation of **2** from the precursor is ca. 3.5×10^{10} s^{-1}, whereas the rate constant for reaction of the precursor with THF is ca. 1×10^{10} M^{-1} s^{-1}, close to the diffusion limit. Assuming that the rate constant for the reaction of the precursor with other nucleophiles (i.e., CO, phosphine, or phosphites) is approximately the same, a 2% reduction in the amount of **2** generated would require the concentration of a nucleophile to be at least 7×10^{-2} M. (The lowest concentration of THF employed in Poliakoff, Turner, and co-workers' experiments is ca. 0.25 M.[4g]) In our experiments, we observe at least a 40% reduction of **2** as compared to the absence of nucleophiles in the presence of CO, phosphine, or phosphites with concentrations on the order of 4×10^{-2} M or lower. This result implies that either the precursor leading to **2** is not as short-lived as believed[4g] or there exists still another precursor which is partly responsible for the formation of **2**. On the basis of the estimated flux of photons in the probe beam, the observed probe beam intensity effect on the production of **2** in our experiments supports the existence of a precursor (or precursors) with a lifetime in the submillisecond domain.

These analyses prompt us to propose other pathways for formation of **2**. One possible pathway is the reaction of $Cp(CO)_2Fe$ and the 15-electron radical Cp(CO)Fe (eqs 7, 9, and 10).

$$Cp(CO)_2Fe \xrightarrow{h\nu} Cp(CO)Fe + CO \quad (9)$$

$$Cp(CO)Fe + Cp(CO)_2Fe \rightarrow Cp_2Fe_2(\mu\text{-}CO)_3 \quad (10)$$

Formation of Cp(CO)Fe is possible via the unsymmetrical cleavage of **1**, eq 7, as well as via secondary photolysis of $Cp(CO)_2Fe$, eq 9. In most experiments by several groups that have observed **2**, continuous photolysis or flash lamp photolysis with UV–visible or IR detection was employed. Under these conditions, secondary photolysis of the $Cp(CO)_2Fe$ radical to form Cp(CO)Fe could occur within the pulse (5 μs or longer) of the lamp flash or could be induced by irradiation from the UV–visible probe beam. The recent finding that **2** is a *secondary* photoproduct from photolysis of $Cp_2Fe_2(CO)_3P(OMe)_3$[4g] may also be explained in terms of reaction of $Cp(CO)_2Fe$ with Cp(CO)Fe.[31]

The presence of CO, phosphorus ligands, and even weak nucleophiles such as $P(C_6F_5)_3$ or THF should suppress the formation of Cp(CO)Fe (eq 11). This is consistent with the observation

$$Cp(CO)Fe + L \rightarrow Cp(CO)FeL \quad (11)$$

that the amount of **2** formed initially is lower in the presence of L. For example, $P(C_6F_5)_3$, a ligand that essentially does not react with **2**, nevertheless suppresses its formation.

It has been shown that the rate constant for recombination of $Cp(CO)_2Fe$ ($k_r = 3 \times 10^9$ M^{-1} s^{-1},[2a] eq 1) is close to the diffusion-controlled limit. Although Cp(CO)Fe is likely to be more reactive than $Cp(CO)_2Fe$, its rate of reaction is nevertheless limited by diffusion. Since in the presence of a nucleophile the concentration ($\sim 10^{-2}$ M) is much greater than that of $Cp(CO)_2Fe$ under the experimental conditions, one would expect that reaction 10 cannot compete with reaction 11. However, when the nucleophile is CO, secondary photolysis from the probe beam, eq 9, competes with reaction 11 during the lifetime of $Cp(CO)_2Fe$. If **2** were produced solely via reaction 10, its formation would be almost completely suppressed in the presence of other nucleophiles, a prediction which is inconsistent with the experimental observations. Furthermore, **2** is observed in recent experiments using laser flash photolysis (308 nm, 30-ns pulse width) with IR detection.[4g] In these experiments, secondary photolysis, eq 9, is unlikely to occur, although a multiphoton process is still possible. We propose that Cp(CO)Fe is one of the precursors leading to formation of **2** as well as **6** but that it is not the only precursor of **2**.

Scheme IV

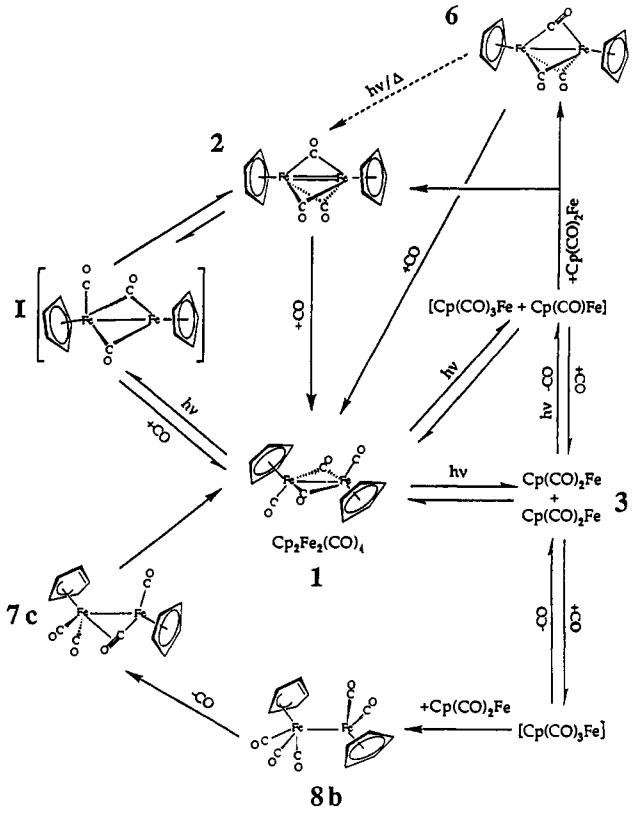

Scheme IV outlines the possible intermediates and processes involved in the photochemistry of **1** in the presence of CO, based on the current understanding of this system. To further reveal the mechanism for formation of **2**, flash photolysis with faster detection techniques is desirable. Utilization of ^{13}CO in such experiments may also be helpful in identifying possible CO exchange via the radical mechanism. **2** was not observed in the femtosecond time-resolved IR experiment by Hochstrasser and co-workers.[6b] However, the use of low-energy (580 nm) laser excitation in these experiments would presumably prelude photodissociation of CO.

Given the current state of fast time-resolved spectroscopy, the traditional methods involving observations at low temperature in matrices or organic media to study reactive intermediates remain very useful. In this report, we have demonstrated an application of low-temperature photolysis and spectroscopy in hydrocarbon media combined with flash photolysis. This approach makes use of the higher sensitivity and resolution of FTIR spectroscopy as compared with time-resolved spectroscopy. Secondly, the use of low-temperature (> −100 °C) solutions permits observations of intermediates resulting from radical processes which could not

(31) In a similar vein to reactions 7 and 8, the symmetrical and unsymmetrical photocleavage of $Cp_2Fe_2(CO)_3P(OMe)_3$ can proceed via reactions 12–14.

$$Cp(CO)Fe(\mu\text{-}CO)_2Fe(Cp)P(OMe)_3 \xrightarrow{h\nu} Cp(CO)_2Fe + Cp(CO)FeP(OMe)_3 \quad (12)$$

$$Cp(CO)Fe(\mu\text{-}CO)_2Fe(Cp)P(OMe)_3 \xrightarrow{h\nu} Cp(CO)_3Fe + CpFeP(OMe)_3 \quad (13)$$

$$Cp(CO)Fe(\mu\text{-}CO)_2Fe(Cp)P(OMe)_3 \xrightarrow{h\nu} Cp(CO)Fe + Cp(CO)_2FeP(OMe)_3 \quad (14)$$

Reaction of $Cp(CO)_2Fe$ with Cp(CO)Fe formed via reaction 12 and 14, respectively, would provide a pathway for the formation of **2** (eq 10).

be observed easily in low-temperature matrices or glasses due to cage effects.

Acknowledgment. This research was supported by the National Science Foundation through grant CHE89-12773.

Supplementary Material Available: Tables of reaction rate constants for **1**, **7**, and **8** at various temperatures and IR data for $Cp_2Fe_2(^{13}CO)_{4-n}(^{12}CO)_n$ (n = 0, 1, 2, 3) in solutions at 25 °C (2 pages). Ordering information is given on any current masthead page.

Reactivity of 17-Electron Organometallic Tungsten and Molybdenum Radicals: A Laser Flash Photolysis Study

Susannah L. Scott, James H. Espenson,* and Zuolin Zhu

Contribution from the Ames Laboratory and Department of Chemistry, Iowa State University, Ames, Iowa 50011. *Received August 27, 1992*

Abstract: Visible (460–490 nm) laser flash photolysis of $[CpW(CO)_3]_2$ or $[CpMo(CO)_3]_2$ induces homolysis of the metal–metal bond with formation of 17-electron radicals, $CpM(CO)_3$. Radical dimerization results in quantitative recovery of the parent dimer and can be followed by the time-resolved increase in dimer absorbance. The reaction follows clean second-order kinetics, $-d[CpM(CO)_3]/dt = 2k_c[CpM(CO)_3]^2$; $k_c(W) = 6.2 \times 10^9$ and $k_c(Mo) = 3.9 \times 10^9$ L mol^{-1} s^{-1} in CH_3CN at 23 °C. The $CpM(CO)_3$ radicals react with organic and inorganic halides and pseudohalides by an atom-transfer mechanism. In the presence of a large excess of the halide-containing substrate, the rate of loss of the radical, $-d[CpM(CO)_3]/dt$, proceeds according to a mixed first- and second-order rate law. The pseudo-first-order rate constants for reactions with organic halides vary linearly with the concentration of the organic halide; bimolecular rate constants for $CpW(CO)_3$ range from 3.9×10^2 L mol^{-1} s^{-1} with CH_2Br_2 to 1.34×10^9 L mol^{-1} s^{-1} for CBr_4. The reactivity trends (RI > RBr > RCl) and (benzyl > allyl > 3° > 2° > 1° > CH_3) are observed. The 7 orders of magnitude variation in bimolecular rate constants is attributed to a highly selective atom abstraction process. The range of rate constants for atom abstraction from halo- and pseudohalopentaamminecobalt(III) and halobis(dimethylglyoximato)cobalt(III) complexes is smaller (2 orders of magnitude, from 1.6×10^7 L mol^{-1} s^{-1} for $NCCo(NH_3)_5^{2+}$ to $>2 \times 10^9$ L mol^{-1} s^{-1} for $BrCo(dmgH)_2py$), because of the upper limit imposed by diffusion. Transfer of the halogen atom from both organic and metal substrates to $CpW(CO)_3$ was confirmed by the IR spectrum of the organometallic product, $CpW(CO)_3X$ (X = Cl, Br, or I). Dioxygen traps $CpW(CO)_3$ with a rate constant $k = 3.3 \times 10^9$ L mol^{-1} s^{-1}. Light-initiated chain reactions were observed at high concentrations of RX, $XCoL_5^{n+}$, or O_2. Hydroperoxides react with $CpW(CO)_3$ by a radical mechanism. The reaction observed between $CpW(CO)_3$ and $(n\text{-}Bu)_3SnH$ is not consistent with either outer-sphere electron transfer or a hydrogen atom abstraction mechanism; oxidative addition to the 17-electron radical is believed to occur in this case. The dimer $[(C_5H_4COOCH_3)W(CO)_3]_2$ shows photoreactivity in organic solvents which is very similar to that of $[CpW(CO)_3]_2$.

Introduction

Mechanisms for organometallic catalysis have been dominated by the 16-/18-electron rule, by which most proposed reactions are formulated with nonradical, even-electron intermediates.[1] However, it is now well-established that some catalytic reactions proceed through organometallic radical intermediates.[2] For example, olefin hydrogenation[3,4] and polymerization[5] are induced by 17-electron radicals. Also, ligand substitution in nonlabile 18-electron complexes can be initiated by formation of 17-electron radicals.[6,7] Although most such radicals are transients, a few 17-electron species are stable toward dimerization. Examples of these are $V(CO)_6$, $Co(CN)_5^{3-}$, $Mn(CO)_3(P(n\text{-}Bu_3))_2$,[8] $Re(CO)_3(PPh_3)_2$,[9,10] and $(C_5Me_5)Cr(CO)_3$.[11]

Formation of 17-electron radicals can be initiated by electron-transfer,[12] electrochemical oxidation[13-17] or reduction[18] and radiolysis[19,20] of metal carbonyl and substituted metal carbonyl monomers and dimers. Also, hydrogen atom abstraction from $HRe(CO)_5$ produces a 17-electron radical.[21] A common initiation step in chain reactions is light-induced metal–metal bond cleavage.[8,22] For $[CpM(CO)_3]_2$ (M = Mo or W), irradiation into either the $d\pi \rightarrow \sigma^*$ or the $\sigma \rightarrow \sigma^*$ transition induces cleavage into 17-electron radicals, $CpM(CO)_3$, as well as CO loss to give $Cp_2M_2(CO)_5$.[23,24] Evidence for the intermediacy of 17-electron radicals includes observation of radical cross-coupling products,[25]

(1) Kochi, J. K. *Organometallic Mechanisms and Catalysis*; Academic: New York, 1978; p 138.
(2) Brown, T. L. In *Organometallic Radical Processes*; Trogler, W. C., Ed.; Elsevier: New York, 1990; Vol. 22, pp 67–107.
(3) Sweany, R. L.; Halpern, J. *J. Am. Chem. Soc.* **1977**, *99*, 8335–8337.
(4) Bullock, R. M.; Samsel, E. G. *J. Am. Chem. Soc.* **1990**, *112*, 6886–6898.
(5) Muetterties, E. L.; Sosinsky, B. A.; Zamaraev, K. I. *J. Am. Chem. Soc.* **1975**, *97*, 5299–5300.
(6) Byers, B. H.; Brown, T. L. *J. Am. Chem. Soc.* **1975**, *97*, 947–949.
(7) Poli, R.; Owens, B. E.; Linck, R. G. *J. Am. Chem. Soc.* **1992**, *114*, 1302–1307.
(8) Kidd, D. R.; Cheng, C. P.; Brown, T. L. *J. Am. Chem. Soc.* **1978**, *100*, 4103–4107.
(9) Moelwyn-Hughes, J. T.; Garner, A. W. B.; Gordon, N. *J. Organomet. Chem.* **1970**, *26*, 373–387.
(10) Singleton, E.; Moelwyn-Hughes, J. T.; Garner, A. W. B. *J. Organomet. Chem.* **1970**, *21*, 449–466.
(11) Watkins, W. C.; Jaeger, T.; Kidd, C. E.; Fortier, S.; Baird, M. C.; Kiss, G.; Roper, G. C.; Hoff, C. D. *J. Am. Chem. Soc.* **1992**, *114*, 907–914.
(12) Krusic, P. J.; Stoklosa, H.; Manzer, L. E.; Meakin, P. *J. Am. Chem. Soc.* **1975**, *97*, 667–669.
(13) Kuivila, H. G. *Adv. Organomet. Chem.* **1964**, *1*, 47–87.
(14) Pickett, C. J.; Pletcher, D. *J. Chem. Soc., Chem. Commun.* **1974**, 660–661.
(15) Treichel, P. M.; Wagner, K. P.; Mueh, H. J. *J. Organomet. Chem.* **1975**, *86*, C13–C16.
(16) Rourke, F.; Gash, R.; Crayston, J. A. *J. Organomet. Chem.* **1992**, *423*, 223–239.
(17) Zhang, Y.; Gosser, D. K.; Rieger, P. H.; Sweigart, D. A. *J. Am. Chem. Soc.* **1991**, *113*, 4062–4068.
(18) Pickett, C. J.; Pletcher, D. *J. Chem. Soc., Dalton Trans.* **1976**, 749–752.
(19) Waltz, W. L.; Hackelberg, O.; Dorfman, L. M.; Wojcicki, A. *J. Am. Chem. Soc.* **1978**, *100*, 7259–7264.
(20) Meckstroth, W. K.; Walters, R. T.; Waltz, W. L.; Wojcicki, A.; Dorfman, L. M. *J. Am. Chem. Soc.* **1982**, *104*, 1842–1846.
(21) Byers, B. H.; Brown, T. L. *J. Am. Chem. Soc.* **1977**, *99*, 2527–2532.
(22) Hallock, S. A.; Wojcicki, A. *J. Organomet. Chem.* **1973**, *54*, C27–C29.
(23) Wrighton, M. S.; Ginley, D. S. *J. Am. Chem. Soc.* **1975**, *97*, 4246–4251.
(24) Hughey, J. L., IV; Bock, C. R.; Meyer, T. J. *J. Am. Chem. Soc.* **1975**, *97*, 4440–4441.

0002-7863/93/1515-1789$04.00/0